A COORDINATED PROCEDURE TO CONTROL HOPF BIFURCATIONS VIA A SECONDARY VOLTAGE REGULATION SCHEME

André A. P. Lerm
UCPel, CEFET-RS
Pelotas, RS, Brazil
alerm@atlas.ucpel.tche.br

Alberto Berizzi
Politecnico di Milano
Milan, Italy
alberto.berizzi@polimi.it

Abstract – This paper presents and discusses a methodology to include in the power system security assessment and control functions a module to deal with oscillatory phenomena, namely Hopf Bifurcations. The proposed procedure is based on the computation of sensitivities of the distance of an operating point of interest to the Hopf Bifurcation in the parameter space, and includes among the control variables the pilot bus voltage of the eventual Secondary Voltage Regulation scheme.

Keywords: Hopf bifurcation, modal analysis, security assessment, security enhancement, secondary voltage regulation.

1 INTRODUCTION

Modern power systems are more and more facing security problems related on one side to the difficulty of building new transmission facilities and on the other side to the presence of the electricity market, which make more and more difficult to plan and operate the system in a coordinated fashion. This is the main reason for the growing uncertainty level which is typically dealt with automatic devices able to face, in real time, scenarios unexpected as for loading level, distribution of generators and loads etc.

One of such automatic controls, which is receiving increasing attention in the world, is the Secondary Voltage Regulation (SVR): it is essentially a control system aimed at maintaining as higher as possible the reactive margins of an area by coordinating the area reactive resources, e.g., the reactive margins of the generators, by controlling the voltage of a "pilot bus" representative of the voltage profiles of that area busses [1]-[6].

The dynamic properties of the power system components, together with their controls, can result in unstable phenomena, which can be studied using the bifurcation approach. Typically, oscillatory phenomena are related to the presence of a Hopf Bifurcation (HB), while, e.g., phenomena like the voltage collapse are linked to the presence of a Saddle Node Bifurcation (SNB). HBs are less frequent than SNBs, but the interest of power system engineers on this issue is growing. In particular, it is of primary interest to understand how to control the distance of a particular operating point to a Bifurcation [7].

The present paper deals with the possibility to control Hopf Bifurcations by adopting a security module that makes use of the sensitivities of such HBs with respect to the set of the control variables. In particular, the original issue is that the set of the control variable can include the control parameters of the SVR, by means of the computation of the suitable sensitivities. After a short introduction to the Bifurcation Theory (Sec.2), the problem of the control of HB is faced in Sec.3, and the implementation of this control in presence of SVR is described in Sec.4. Sec.5 provides some examples of the proposed methodology based on the New England test system, and Sec.6 concludes on the results obtained and on future research activity.

2 BACKGROUND

This section explains some basic aspects necessary to define the methodology proposed in the paper to control a power system in order to avoid oscillatory problems.

2.1 System Model

Nonlinear dynamical systems, such as those obtained from certain power system models, can be generically described by the following ordinary differential equation (ODE) system:

$$\dot{\boldsymbol{x}} = \boldsymbol{f}(\boldsymbol{x}, \lambda) \qquad (1)$$

where $\boldsymbol{x} \in \Re^n$ is the state variables vector (e.g., state variables corresponding to a series of system devices, such as generators, and their controls); $\lambda \in \Re^{k+1}$ represents the set of parameters; in the paper, in particular, $\lambda=[\mu\ \boldsymbol{p}]^T$, where μ represents a real loading "non controllable" scalar parameter (i.e., the loading pattern of the system is assumed fixed); $\boldsymbol{p} \in \Re^k$ represents a set of "controllable" parameters (e.g., AVR set points, shunt compensation or load shedding); and $\boldsymbol{f}: \Re^n \times \Re^{k+1} \rightarrow \Re^n$ is a non-linear vector function.

Moreover, typical power system models used in stability analysis present an additional difficulty, as these systems are modeled with a set of differential and algebraic equations (DAE) of the form

$$\begin{bmatrix} \dot{x} \\ 0 \end{bmatrix} = \begin{bmatrix} \boldsymbol{f}(\boldsymbol{x}, \boldsymbol{y}, \lambda) \\ \boldsymbol{g}(\boldsymbol{x}, \boldsymbol{y}, \lambda) \end{bmatrix} = \boldsymbol{F}(\boldsymbol{z}, \lambda) \qquad (2)$$

where the notation adopted for $\boldsymbol{x}$, and λ is the same as for (1); in addition, $\boldsymbol{y} \in \Re^m$ represents the set of algebraic variables defined by the nonlinear algebraic function $\boldsymbol{g}: \Re^n \times \Re^m \times \Re^{k+1} \rightarrow \Re^m$ (which typically correspond to load bus voltages and angles, depending on the load models used), the function $\boldsymbol{f}$ is re-defined as $\boldsymbol{f}: \Re^n \times \Re^m \times \Re^k \rightarrow \Re^n$, $\boldsymbol{F} = [\boldsymbol{f}, \boldsymbol{g}]^T$ and $\boldsymbol{z} = [\boldsymbol{x}, \boldsymbol{y}]^T$.

The stability of DAE systems is thoroughly discussed from the theoretic point of view in [8]. A practical analysis of (2), however, is based on the eigenvalue computation of the Jacobian calculated at an equilibrium point defined by the subscript o:

$$\boldsymbol{A} = D_{\boldsymbol{x}} \boldsymbol{f}\,|_o - D_{\boldsymbol{y}} \boldsymbol{f}\,|_o\,(D_{\boldsymbol{y}} \boldsymbol{g}\,|_o)^{-1} D_{\boldsymbol{x}} \boldsymbol{g}\,|_o \qquad (3)$$

In the following, the Jacobian defined in (3) will be studied to identify suitable control actions to avoid instability problems.

2.2 Equilibria and Steady-State Points

The system equilibria obtained from $\boldsymbol{F}(\boldsymbol{z}_o,\boldsymbol{\lambda}_o)=0$ are typically defined through a subset of equations referred to as the conventional power flow equations. Hence, the typical procedure is to first solve the power flow equations and then find equilibrium points of the dynamic model before proceeding with the stability analysis of the full DAE system (2). For some particular dynamic models and power flow models [9], there is no need to solve the full system (2), but the solution of the power flow equations is sufficient. However, for most realistic models, the solution of the power flow equations is not coincident with the steady state solution of (2). An example is given by the computation of the so called PV curves when only the power flow equations are used [10]. Usually, a generator is assumed to have a constant terminal voltage in the load flow model (PV bus); however, if the corresponding AVR is modeled in detail, the voltage set-point for this controller should change at each point on the PV curve to account for voltage droop, and hence keep the terminal voltage constant.

In the present work the equilibrium points are computed by the solution of (2), considering constant set-points of AVRs and governors. This procedure allows the obtained PV curves to be consistent with the bifurcation diagrams of (2) [11].

2.3 Local Bifurcations

Standard bifurcation theory deals with the study of the stability of ODE systems (1) that move from equilibrium to equilibrium as the parameter μ slowly changes [12][13]; these concepts can be directly extended to DAE systems represented by (2) [14]. There are several types of bifurcations associated with the changes of μ, some local and some global, depending on the behavior of the system dynamic manifolds and equilibrium points. The present paper concentrates only on the analysis of local bifurcations, in particular the Hopf Bifurcation (HB), which can be detected and analyzed by monitoring the eigenvalues of the Jacobian defined in (3).

The HB is characterized by a complex conjugate pair of eigenvalues crossing the imaginary axis of the complex plane as μ slowly changes. This type of bifurcation has been associated with a variety of oscillatory phenomena in power systems [7].

3 CONTROL OF HOPF BIFURCATION

The analysis of HB is related to the possibility to obtain a proximity index; the sensitivities of the distance of the current operating point to the HB can be used to control the power system in order to define a new operation point more secure with respect to such instability risk.

First, the basic concepts on the computation of HB sensitivities are briefly resumed from [15]. The analysis developed in that paper, however, is based on the ODE representation (1) for the power system. As large power systems are usually represented through a DAE system like (2), it is necessary to modify the original methodology. In the following, the original and the adapted methodologies are presented.

3.1 Sensitivity of Hopf Bifurcation for ODE systems

Assume that when the loading parameter μ slowly increases to a critical value μ_* and the design parameters are fixed at $\boldsymbol{p_0}$, the system loses stability in a HB. The loading margin to instability is then $M=\mu_*-\mu_0$. However, the loading margin M can be increased by controlling $\boldsymbol{p}$ through the use of the sensitivity $\boldsymbol{M_p}|_{p0}$.

The sensitivity $\boldsymbol{M_p}|_{p0}$ is essentially a scaled projection of a normal vector to the HB hypersurface Σ^{Hopf}. A normal vector [15] to Σ^{Hopf} is given by the sensitivities of the real part with respect to the parameters as

$$\boldsymbol{N}(\boldsymbol{\lambda}_*) = \mathrm{Re}\{\boldsymbol{\omega}^T (\boldsymbol{f}_{xx}\boldsymbol{u}_\lambda + \boldsymbol{f}_{x\lambda})\boldsymbol{v}\} \qquad (4)$$

where $\boldsymbol{v}$ and ω are the normalized right and left eigenvectors of the Jacobian matrix $\boldsymbol{f_x}|_*$ corresponding to the complex pair of eigenvalues on the imaginary axis (the normalization is such that $|\boldsymbol{v}|=1$ and $\omega^{\mathrm{T}}\boldsymbol{v}=1$), $\boldsymbol{f_{xx}}$ is an $n\times n\times n$ tensor, $\boldsymbol{f}_{x\lambda}$ is an $n\times n\times(k+1)$ tensor and $\boldsymbol{u}_\lambda$ is the $n\times(k+1)$ Jacobian of $\boldsymbol{f}$ with respect to the control variables $\boldsymbol{\lambda}$.

The sensitivity of the load margin with respect to the k controllable parameters $\boldsymbol{p}$ is given by the scaled vector:

$$\boldsymbol{M_p}\Big|_{\boldsymbol{p}0} = -n_\mu^{-1}[n_{p1} \quad n_{p2} \quad \ldots \quad n_{pk}] \qquad (5)$$

where n_i are the elements of $\boldsymbol{N}(\boldsymbol{\lambda}_*)$ (assuming $n_\mu\neq 0$).

3.2 Sensitivity of Hopf Bifurcation for DAE systems

The sensitivity of HB theory presented above is straightforward for ODE systems. However, when a power system is represented by a DAE system (2), the Jacobian $\boldsymbol{f_x}$ should be replaced by the matrix $\boldsymbol{A}$ of (3); if the problem involves only the determination of bifurcation diagrams, the use of $\boldsymbol{A}$ does not represent a great challenge. On the other hand, since $\boldsymbol{A}$ is not obtained explicitly, the sensitivity analysis is very laborious because the cubic matrices $\boldsymbol{A_x}$ and $\boldsymbol{A}_\lambda$ should be computed. In order to avoid this problem, the present work uses the methodology suggested in [16] and applied in [17], which is based on the use of the "extended" right and left eigenvectors, $\boldsymbol{e}=[\boldsymbol{e}_1\ \boldsymbol{e}_2]^{\mathrm{T}}$ and $\boldsymbol{d}=[\boldsymbol{d}_1\ \boldsymbol{d}_2]^{\mathrm{T}}$ respectively, associated to the eigenvalue σ.

The "generalized" eigenvalue problem of (2) can be stated [16] as

$$\begin{bmatrix} \sigma \boldsymbol{e}_1 \\ 0 \end{bmatrix} = \begin{bmatrix} D_x \boldsymbol{f} & D_y \boldsymbol{f} \\ D_x \boldsymbol{g} & D_y \boldsymbol{g} \end{bmatrix} \begin{bmatrix} \boldsymbol{e}_1 \\ \boldsymbol{e}_2 \end{bmatrix}$$

Using the concept of "extended" eigenanalysis, the sensitivity of HB can be determined for the DAE system (2), as [17]:

$$\boldsymbol{N}(\lambda_*) = \mathrm{Re}\{\boldsymbol{d}^{\mathrm{T}}(\boldsymbol{F}_{zz}\boldsymbol{u}_{\lambda} + \boldsymbol{F}_{z\lambda})\boldsymbol{e}\} \quad (6)$$

where now $\boldsymbol{u}_\lambda$ is the matrix of the derivatives of $\boldsymbol{F}$ with respect to the control variables $\boldsymbol{\lambda}$.

3.3 The Secondary Voltage Regulation for the control against a Hopf Bifurcation

Under normal conditions, the main objective of the system control is to operate as efficiently as possible with voltages and frequency close to their nominal values. Regarding the voltage at busbars, this goal is achieved primarily by controllers such as AVRs, LTC transformers and reactive power compensation devices and, at a hierarchical higher level, if available, by a SVR scheme, with a slower time constant. However, if the system margin regarding a specific bifurcation is unsafe, the SVR can be employed to meet new objectives such as restoring a system security acceptable level [5].

The SVR is a control scheme designed to manage voltage profiles and reactive power [1]-[5]. In general, this control can act on the set-point of AVRs, the switching of compensation devices and the change of tap position on transformers [4]. The present work assesses the possibility to use the additional signals available from the SVR in order to postpone an oscillatory instability caused by a HB. The main idea of the proposed methodology is that, if a stability margin is greater than a minimum specified, then the SVR acts in order to obtain an optimal voltage profile for the system. On the other hand, if it operates with an unsafe margin, the SVR is used to obtain a new voltage profile associated to a better stability margin.

The SVR is currently adopted in France and in Italy, with slightly different implementations. In Italy, e.g., a hierarchical voltage control system [2] is based on the presence of three levels: the AVRs are the fist level, the SVR is the second level and the Tertiary Voltage Regulation (TVR) is the third one. The Italian system is divided into several areas (about 18, at the moment) and each area has to provide the reactive power necessary to control the voltage of the bus representative of the entire area: the pilot bus. The reactive power to be produced by each area is shared among the controlling generators of that area in such a way that the reactive loading is equal in p.u. for each controlling generator. This makes more secure the power system against possible perturbations. The TVR level is designed to reschedule online the set points of the pilot nodes to account for differences between the forecasted and the actual system state.

This paper is mainly dealt with a different use of the SVR, in order to make the system more secure against oscillatory phenomena. For this reason, a simpler scheme will be adopted for the SVR: Fig. 1 presents the block diagram for the SVR used in this work. It is essentially the same as indicated in [6], differing only by the inclusion of limiter functions. This scheme includes two main parts: *i)* a central controller, which acts in order to control the voltage at the pilot-node, and *ii)* a power plant controller, which regulates the reactive power output of the plants participating on the scheme.

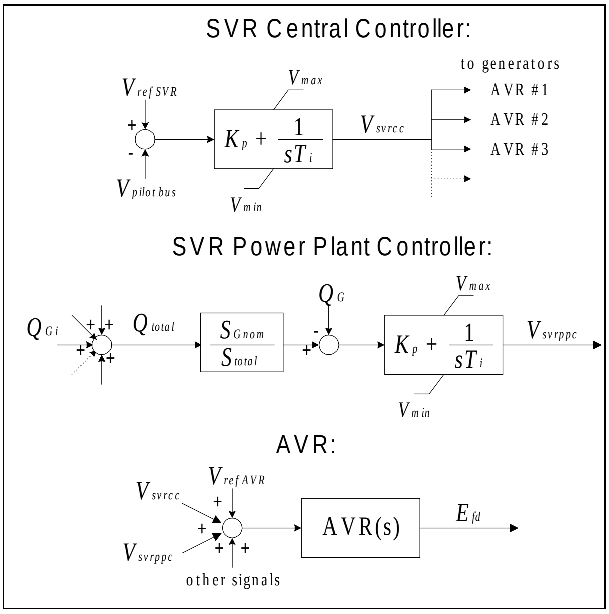

Figure 1: SVR control scheme.

The above scheme allows the demonstration of the feasibility of the proposed methodology in order to improve the system security against HBs, following the ideas in [17]. That work addressed the sensitivity analysis of the HB regarding a possible reschedule of set-points of AVRs while their numerical results showed the potentiality of this methodology. The present work includes a SVR scheme in the analysis and presents a coordinated procedure to control HBs based on it. The following section explains some aspects related to this new methodology.

4 THE COORDINATED PROCEDURE TO CONTROL HOPF BIFURCATIONS

The proposed methodology has two important modules: the evaluation of the stability margin to HBs and the improvement of this margin based on a reactive power redispatch of generators.

4.1 The Hopf bifurcation evaluation module

For the determination of the stability margin, a known pattern of load increase must be assumed. Starting from an initial equilibrium point, the load is increased by an automatic procedure based on variable steps on the parameter μ. These steps are refined up to a pre-selected value represented by the numerical precision desired for the bifurcation point. When a HB is detected, by monitoring the eigenvalues of the matrix $\boldsymbol{A}$ of

(3), the stability margin of the base case is defined as the distance of this bifurcation point in terms of μ. If this margin is below a threshold, the security enhancement procedure takes place.

The modeling of limits, such as those applied to the field voltage E_{fd} of AVRs, plays an important role in the searching process of the HB point. The procedure takes into account a complete modeling of limits, as indicated in [18]. If a limit is hit, a sudden change on the system behavior takes place, and a Limit Induced Bifurcation (LIB) can occur [11]: the complex pair of eigenvalues related to the HB can be destroyed when limits are reached. Two important consequences can follow: *a)* If the LIB is stable, depending on the step used for the iteration which detects the limitation, the searching process must verify with a smaller step the existence of a HB before the LIB; if there is no such bifurcation, the Hopf searching process continues for a loading level upper the LIB point. *b)* If the LIB is unstable, an immediate instability is verified as consequence of the limitation; in this case, the phenomenon needs a specific analysis based on its hypersurface and thus it is not covered by this work.

4.2 The security enhancement module

Once a HB has been detected, the enhancement module takes place to determine the preventive or corrective actions required to increase the security margin and to postpone the HB, using as control variables, in addition to the traditional ones, the signals controlled by the SVR scheme. Table 1 indicates four different options implemented in this module. In this table, SVRCC and SVRPPC refer to the central and the power plant controllers (Fig. 1).

Option	SVRCC	SVRPPC	Control param. (p)
1	enabled	enabled	$V_{ref\,SVR}$
2	enabled	disabled	$V_{ref\,SVR}$
3	disabled	enabled	$V_{svrcc\,i}$
4	disabled	disabled	$V_{svrppc\,i}$

Table 1: Different options for the Hopf control via a SVR scheme.

There are significant differences between the options presented here. For those with the SVRCC enabled, the resultant scheme, in addition to the Hopf control, acts in order to keep constant the voltage at the pilot busbar. For SVRPPC enabled there is a regulation on the reactive power output of the plants participating on the SVR. The implementation considers also that, if the disabled controller is not related to the control parameter p_i, then the associated signal is kept constant in the simulations. Some of those options are more realistic: for example, Option 1 means SVR fully in operation, while Option 4 is relevant to the absence of SVR. As a result of the application of this methodology, the resulting secure operating point is characterized by a new voltage profile, kindly different from the one obtained with the original setting of the SVR.

The following section presents some numerical results for the methodology presented here.

5 NUMERICAL RESULTS

The present section applies the proposed methodology to the New England test system [19]. In all simulations performed, the bifurcation parameter μ is used to model power load variations in all buses, i.e., $\boldsymbol{P}_l=\boldsymbol{P}_{lo}(1+\mu)$ and $\boldsymbol{Q}_l=\boldsymbol{Q}_{lo}(1+\mu)$, where $\boldsymbol{P}_{lo}$ and $\boldsymbol{Q}_{lo}$ are the initial values for the loads. All loads are considered independent on the voltage, for both active and reactive power. The bifurcation diagrams are determined directly from the DAE system, with the use of constant set-points of AVRs and governors (values indicated in Appendix). In order to perform a realistic simulation, an Automatic Generation Control (AGC) is added to the original system. The AGC allows a constant frequency for the system when the demand load is increased according to μ. The input signal of this AGC is the frequency deviation while the output acts uniformly on the generators 32 to 39.

The SVR scheme considered for this system is made by only one area: this allows the easy evaluation of the improvement of the security against HBs, even if possible interactions among areas are not considered. The considered area is relevant to the pilot bus 19, controlled by generators 31 to 34. The pilot busbar voltage set point is $V_{ref\,SVR}$ = 1.02 p.u. The choice for this node as the pilot busbar is justified by its strong influence on the voltage of the remaining busbars. The parameters adopted for this SVR are K_p=0.005 and T_i=100.0 s, for both central and power plant controllers.

Referring to the following figures, the behavior of the system under SVR action is such as indicated by the curves which include the points A and A1. At the point A1, the system experiences the HB, with the loading μ=0.1748. The complex pair of eigenvalues associated to this Hopf has an imaginary part around 2.5 rad/s; a participating factor analysis indicates an association of this pair mainly with the variables E'_q and E_{fd} of generator 38. In order to control this bifurcation, a secure margin on μ=0.02 is adopted. This margin allows the system to have a damping factor associated to the dominant eigenvalues greater than 0.085. Therefore, for a loading parameter greater than μ=0.1548, indicated in the figures by the point A, the control procedure described in the previous sections becomes active, to improve the security margin. For the sake of brevity, only the results of the Options 1 and 4, accordingly to Table 1, are shown in the following.

5.1 Option 1

When the control is operating with Option 1, both central and power plant controllers are enabled, and the set-point $V_{ref\,SVR}$ of the SVR is the only control parameter. The results obtained in this case are shown in Figures 2 and 3, where the voltage at busses 16 and 19 (pilot busbar), respectively, are plotted as function of μ.

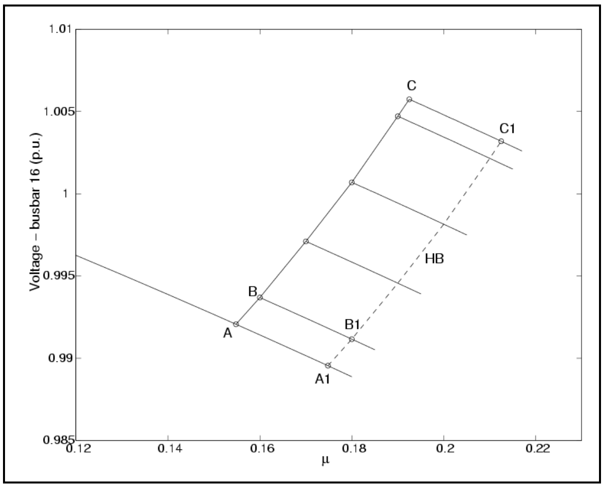

Figure 2: Bifurcation diagrams obtained for HB control with Option 1.

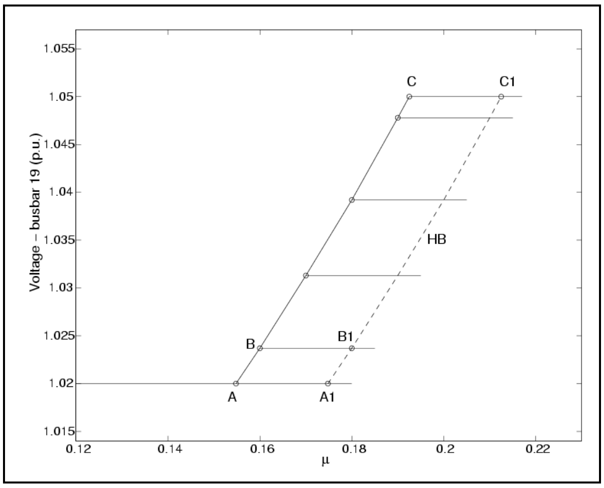

Figure 3: Bifurcation diagrams obtained for HB control with Option 1.

Figures 2 and 3 explain some details of the adopted control. Consider the search of the optimal set-point V_{refSVR} regarding the stability margin for the loading μ=0.16, starting with the original set-point $V_{ref\,SVR}$ = 1.02 p.u. From the loading μ=0.16, the HB evaluation module increases the load up to the Hopf point. Since the HB occurs at point A1 (μ=0.1748), the system has a margin M=0.0148. In order to increase the margin from 0.0148 to 0.02, the security enhancement module is called. The aim of the control is then to add a margin 0.0052 to the original 0.0148, based on the sensitivity computed for the HB point. As the sensitivity of M with respect to the set-point $V_{ref\ SVR}$ is equal to 1.4010, it follows that this set-point should be increased by 0.0052/1.4010=0.0037. Once the pilot bus voltage is updated, with the new $V_{ref\,SVR}$ = 1.0237 the procedure is iterated until the pre-selected margin M=0.02 is attained. In this particular case, one iteration is sufficient to obtain the desired security margin and the procedure gives, for μ=0.16, the new point B, to which corresponds a HB point (B1) for μ=0.18. Also, voltage at bus 16 is higher than the voltage in A and it is equal to 0.9937. If the mentioned procedure is applied to different loading values, the resulting set of equilibrium points describes the curve evolving the points A-B-C. The last point C corresponds to the upper limit of V_{refSVR} equal to 1.05. Notice that if $V_{ref\,SVR}$ is kept constant from any point on the curve A-B-C, the system experiences the Hopf at the curve HB. The fact that only one iteration is sufficient indicates that the non-linearity of the system is not remarkable. This is confirmed by other tests: usually three iterations are enough to reach the goal of the security enhancement module.

5.2 Option 4

With this option, both central and power plant controllers are disabled. Consequently, when the HB control scheme starts, the signal V_{svrcc} from the central controller is kept constant and the signals $V_{svrppc\ i}$ from the power plants are considered the controllable parameters. The results obtained in this case are shown in Figures 4 and 5.

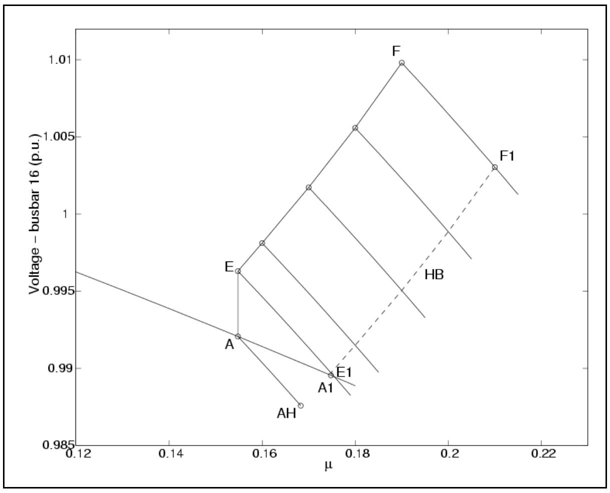

Figure 4: Bifurcation diagrams obtained for HB control with Option 4.

Since this HB control scheme disables the original blocks of the central and power plant controllers, the resulting switching of equations change the HB originally detected without it. In fact, for the point A depicted on Figures 4 and 5 a new HB is detected at a lower loading level μ=0.1683 (point AH): this demonstrates that the only presence of the SVR (Option 1) gives a higher margin with respect to the HB. Suppose the system is working at a loading level μ=0.1548, and thus the security margin is not guaranteed. In order to control it, the operating point should be changed to point E, at a higher voltage level (V_{16}=0.9963, V_{19}=1.0269), to which corresponds the HB (point E1) at the loading level μ=0.1748. As a consequence, in order to maintain the desired stability margin for the system, a new operating point E (with a higher value of voltage) is obtained for the loading μ=0.1548. Notice also that there is no more a constant voltage for the pilot busbar, as indicated in Figure 5.

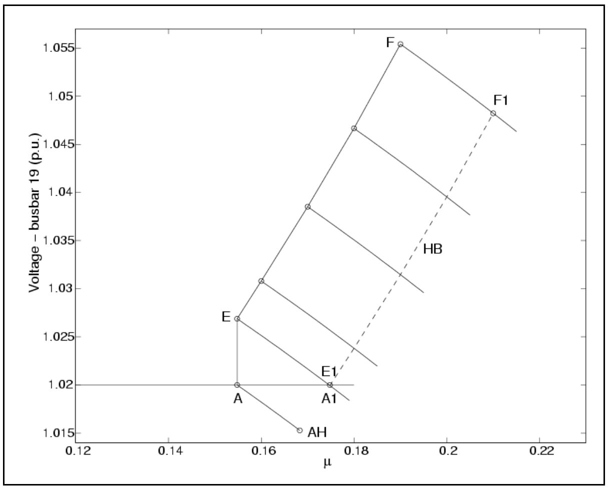

Figure 5: Bifurcation diagrams obtained for HB control with Option 4.

5.3 Influence on other bifurcations

Other bifurcations than HB present in the system affect the use of the proposed methodology. Figure 6 shows in detail other bifurcations present in the simulation when Option 1 is performed and there is no limitation applied to $V_{ref\,SVR}$. After the HB, the system experiences an unstable LIB, associated to the Q limitation of the generator 34. This LIB occurs on the curve which includes the points A2-C2-D2 and is followed by the saddle-node bifurcation, indicated by the point SNB. One can see clearly that the HB curve is destroyed at the point D1, when it reaches this unstable LIB manifold. As a consequence, for loadings greater than μ=0.2010 with $V_{ref\,SVR}$=1.0580 (point D) the HB evaluation module does not detect the HB.

A detailed set of bifurcation diagrams for the Option 4 is shown in Figure 7. These manifolds were obtained by simulations without limits applied to the signals V_{svrppc} of each generator. Differently from the previous case, the LIB that follows the HB is now a stable one and hence there is no more an immediate change in the stability when machine 34 reaches its limits. However, an interesting event occurs for loadings upper than that related to the point G, with μ=0.2200. For this point, the coordinated procedure to control the HB brings the system to the HB at the point G1, with μ=0.2400. At this point however, the HB manifold reaches the stable LIB curve, and there is a "jump" on the eigenvalues related to the HB. A new Hopf point is then obtained at the point HB*, with μ=0.2466. The possibility of this increase on the system margin as consequence of a LIB occurrence must be considered by the proposed coordinated procedure.

Regarding the results obtained here, it must be emphasized that they are specific for this particular system. These results, however, demonstrate the importance of the evaluation and comparison of several options in order to obtain a reliable control on the system.

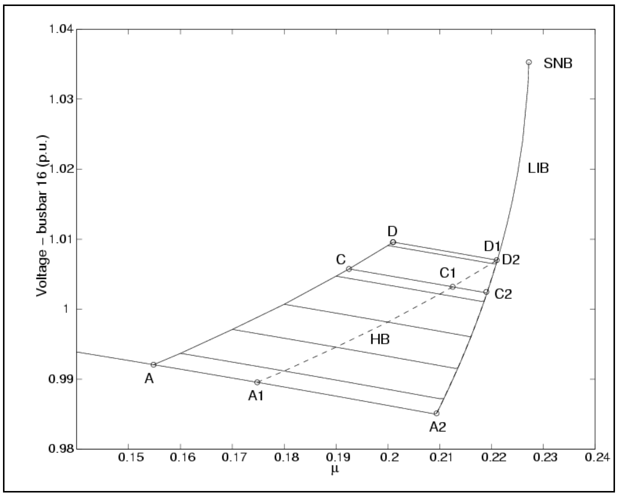

Figure 6: Detailed bifurcation diagrams for Option 1.

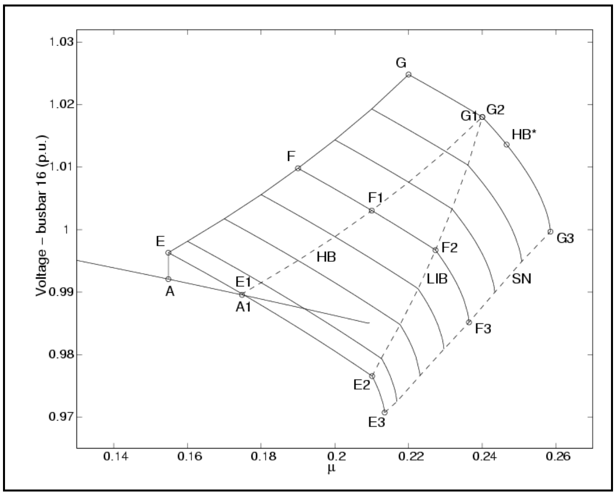

Figure 7: Detailed bifurcation diagrams for Option 4.

6 CONCLUSIONS

This paper presents and discusses a coordinated procedure to control Hopf bifurcations in electric power systems based on the additional signals available from a Secondary Voltage Regulation (SVR) scheme. This procedure comprises the modules related to the evaluation of the stability margin to the Hopf bifurcation point and the improvement of this margin based on a reactive power redispatch of generators. The resulting secure operating point is characterized by a new voltage profile, kindly different from the one obtained with the original setting of the SVR.

The results presented for the New England test system demonstrate the effectiveness of the proposed methodology on the control of Hopf bifurcation.

Future work on this subject includes the application of the proposed methodology to a real multi-area system.

REFERENCES

[1] P. Lagonotte, J. C. Sabonnadière, J. Y. Léost and J. P. Paul, "Structural Analysis of the Electrical System: Application to Secondary Voltage Control in France", IEEE Transactions on Power Systems, Vol. 4, No. 2, pp. 479-486, May 1989.

[2] S. Corsi, P. Marannino, N. Losignore, G. Moreschini, G. Piccini, "Coordination between the reactive power scheduling function and the hierarchical voltage control of the EHV ENEL system", IEEE Trans. on Power Systems, vol.10, no.2, pp.686-694, May 1995.

[3] A. Berizzi, P. Bresesti, P. Marannino, G. P. Granelli, M. Montagna, "System-area operating margin assessment and security enhancement against voltage collapse", IEEE Transactions on Power Systems, vol.11, n.3, pp.1451-1462, Aug.1996.

[4] H. Vu, P. Pruvot, C. Launay and Y. Harmand, "An Improved Voltage Control on Large-Scale Power System", IEEE Transactions on Power Systems, Vol. 11, No. 3, pp. 1295-1303, Aug. 1996.

[5] A. Berizzi, A. Bignotti, P. Finazzi, D. Dosi and P. Marannino, "An Automatic Procedure for Evaluating and Improving Operating Margins Against Voltage Collapse", *12nd Power Systems Computation Conference*, 1996.

[6] N. Martins et all, "A Demonstration Example of Secondary Voltage Regulation: Dynamic Simulation and Continuation Power Flow Results", Proceedings of the IEEE PES-SM, Vancouver, CA, July 2001.

[7] C. Cañizares, ed., "Voltage Stability Assessment, Procedures and Guides," IEEE/PES Power System Stability Subcommittee Special Publication, Final Draft, http://www.power.uwaterloo.ca, Dec. 2000.

[8] D. J. Hill and I. M. Y. Mareels, "Stability Theory for Differential/Algebraic Systems with Application to Power Systems", IEEE Trans. Circuits and Systems, Vol. 37, No. 11, pp. 1416-1423, Nov. 1990.

[9] I. Dobson, "The irrelevance of load dynamics for the loading margin to voltage collapse and its sensitivities", Proc. Bulk Power System Voltage Phenomena III-Voltage Stability and Security, ECC Inc., pp. 509-518, Aug. 1994.

[10] B. C. Lesieutre, P. W. Sauer and M. A. Pai, "Why Power/Voltage Curves Are Not Necessarily Bifurcation Diagrams", 25th North American Power Symposium, Washington, pp. 30-37, Oct. 1993.

[11] A. A. P. Lerm, C. A. Cañizares, F. A. B. Lemos and A. S. e Silva, "Multi-parameter Bifurcation Analysis of Power Systems", 31st North American Power Symposium, Cleveland, Oct. 1998.

[12] R. Seydel, "Practical Bifurcation and Stability Analysis-From Equilibrium to Chaos", Second Edition, Springer-Verlag, New York, 1994.

[13] J. Guckenheimer and P. Holmes, "Nonlinear Oscillations, Dynamical Systems and Bifurcation of Vector Fields", Applied Mathematical Sciences, Springer-Verlag, New York, 1986.

[14] H. G. Kwatny, R. F. Fischl, and C. O. Nwankpa, "Local Bifurcation in Power Systems: Theory, Computation, and Application", Proceedings of the IEEE, Vol. 83, pp. 1456-1483, Nov. 1995.

[15] I. Dobson, F. Alvarado and C. L. De Marco, "Sensitivity of Hopf Bifurcations to Power System Parameters", Proc. of the 31st Conference on Decision and Control, Tucson, Arizona, pp. 2928-2933, Dec. 1992.

[16] T. Smed, "Feasible Eigenvalue Sensitivity for Large Power Systems", IEEE Transactions on Power Systems, Vol. 8, No. 2, pp. 555-563, May 1993.

[17] A. A. P. Lerm and A. S. e Silva, "The Use of Voltage Profile on Oscillatory Instability Control", 33rd North American Power Symposium, Waterloo, ON, Canada, Oct. 2000.

[18] A. A. P. Lerm, C. A. Cañizares and N. Mithulananthan, "Effects of Limits in Small Signal Stability Analysis of Power Systems", Proceedings of the IEEE PES-SM, Vancouver, CA, July 2001.

[19] "Frequency Domain Analysis of Low Frequency Oscillations in Large Electric Power Systems", Interim Report El-726, EPRI, 1978.

APPENDIX

Gen	V_{ref} (p.u.)	$P_{mec\ ref}$ (MW)
30	1.0241	250.107
31	0.9363	583.600
32	1.0221	651.856
33	0.9611	632.918
34	1.1787	508.391
35	1.0090	676.061
36	1.1347	560.767
37	0.9884	541.893
38	1.0915	831.961
39	1.0605	1000.974

Table 2: Set-points of AVRs and governors.